# Modulation of Aluminum Species in Mordenite Zeolite for Enhanced Dimethyl Ether Carbonylation

Yunduo Liu [a, b,1], Ying Li [a, c,1], Ji Qi [d], Hu Liu [a], Xiaodong Wang [e], Shiwei Wang [b], Kongying Zhu [f] *, Shouying Huang [a, b] * and Xinbin Ma [a]

[a] *Key Laboratory for Green Chemical Technology of Ministry of Education, Haihe Laboratory of Sustainable Chemical Transformations, School of Chemical Engineering and Technology, Tianjin University, Tianjin, 300350, China*

[b] *Zhejiang Institute of Tianjin University, Ningbo, 315201, China*

[c] *College of Chemical Engineering, Inner Mongolia University of Technology, Hohhot, 010051, China*

[d] *Institute of Molecular Plus, Tianjin University, Tianjin, 300072, China*

[e] *Chemical Engineering, School of Engineering, Lancaster University, Lancaster LA1 4YW, United Kingdom*

[f] *Nuclear Magnetic Resonance Test Center, Tianjin University, Tianjin, 300350, China*

## Corresponding author

* Kongying Zhu: ausky@tju.edu.cn; Shouying Huang: huangsy@tju.edu.cn;

## Abstract

Dimethyl ether (DME) carbonylation is an important intermediate step in the synthesis of methyl acetate (MA) and ethanol. H-form mordenite (MOR) can efficiently catalyze the reaction, in which Brønsted acid sites (BASs) associated with framework Al function as active sites. But the role of other Al species such as exteraframework Al (EFAl) and framework-associated Al still remains unknown. In this study, we have proposed two convenient approaches for controlling the two Al species and investigating their influence on the DME carbonylation reaction. $NH_3$-TPD and Py-IR analyses revealed that the number of BASs increased after the removal of EFAl and the inhibition the formation of framework-associated Al. The reactivity results showed that the elimination of EFAl promoted the DME conversion from 28 % to 46 %. Additionally, through the implementation of in-situ calcination to impede the presence of framework-associated Al, the DME conversion increased from 28 % to 50 %. With the understanding that both EFAl and framework-associated Al have a detrimental effect on the reaction, the highest conversion is achieved with these two treatments, leading to 73 % DME conversion with 99 % selectivity to MA. Our findings provide a systematical strategy to effectively regulate the presence of Al species in zeolite, offering insights of rational design to optimize zeolite catalysts for important industrialized process.

Keywords: DME carbonylation reaction; mordenite; extraframework Al; framework-associated Al.

## 1. Introduction

Ethanol is a large-scale chemical being widely used as feedstock, solvent, and fuel additive as well as alternative transportation fuel. Currently, ethanol is mainly synthesized through biomass fermentation [1] and ethylene hydration [2]. Due to threatening of food supplement and heavily petroleum usage, the development of green and efficient routes for ethanol production based on alternative resources has drawn more and more attention. Recently, a new route has been developed which relies on converting carbon source (such as coal, biomass) into syngas has been developed. This route involves carbonylation of dimethyl ether (DME) to methyl acetate (MA) followed by hydrogenation to produce ethanol. Due to the high atom economy and the absence of ethanol and water azeotrope in the product, it has been received increasing recognition from both academia and industry [1, 3, 4].

As a critical intermediate step for ethanol synthesis, DME carbonylation could be achieved by using sold acid catalysts such as zeolites [5]. Mordenite (MOR) consisting of 8 membered ring (8-MR) channel and 12-MR channel exhibits a superior DME carbonylation reactivity [6]. The active sites for DME carbonylation reaction are believed to be the Brønsted acid sites (BASs) within 8-MR due to its unique spatial configuration [7], which balance the negative charges derived from the framework Al. In addition to framework Al, extraframework Al (EFAl) is also commonly present in zeolites, which may affect the acidic property thus have a vast impact on the catalytic performance. Therefore, it is important to regulate the Al species in MOR and identifying their roles in the DME carbonylation.

EFAl exists in the form of several oxides and hydroxides, such as $Al^{3+}$, $Al(OH)^{2+}$, AlOOH, $Al_2O_3$, $Al(OH)_3$ [8-11]. Under steaming or high-temperature conditions, or chemical treatment, EFAl could be generated through Si-O-Al bonds hydrolysis [8, 12, 13]. Wang et al. found that the EFAl generated in β zeolite by the acid treatment was able to strengthen the BASs acidity, thus presenting a higher conversion in n-octane cracking [14]. On the contrary, Gounder et al. found that the removal of EFAl increased the pore size of the USY zeolite without changing the acid strength. As a result, the reaction intermediate (i.e. protonated $CH_3OH$ dimers) is less restricted and the methanol dehydration reactivity is promoted [15]. Xue et al. found that the EFAl in ZSM-5 decreased the intrinsic entropy change of n-pentane cleavage, thus promoting the cracking rate [16]. And in isobutane cracking reaction, the tertiary C−H bond in isobutane selectively activated solely on EFAl, while the C−C bond could be activated by BASs [17].

However, when researchers attempt to correlate the EFAl to Lewis acidity, it was found that there is no recognized conclusion on the relationship [10]. This is because EFAl and framework-associated Al have an overlap characteristic feature from NMR technique limiting the rational correlation built-up. As shown in Scheme 1, framework-associated Al is derived from the transformation of framework aluminum by interaction with water at room temperature which exhibits hexacoordination state, and after ammonia ion-exchange, framework-associated Al is transformed to framework Al (tetrahedrally coordination) [18-20]. Thus, the generation of framework-associated Al leads to the decrease of BASs and therefore affects the catalytic reaction performance.

However, the understanding of EFAl and framework-associated Al influence on DME carbonylation reactivity is still not deep researched and the regulation of specific Al species to further well-control the carbonylation reactivity is lack of investigation.

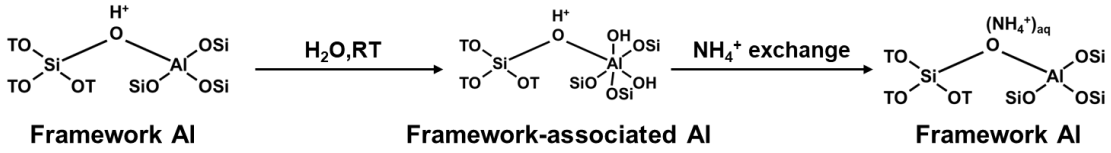


Scheme 1. Schematic of the evolution of Al species in MOR

In this work, we use sodium ethylenediaminetetraacetic acid disodium salt (EDTA-2Na) and in-situ calcination to modify Al species within MOR and establish the structure-performance relationship on DME carbonylation reaction. We proposed that the EDTA-2Na is capable of removing EFAl without destroying zeolite structure leading to more exposed Brønsted acid sites and therefore promoting the DME conversion from 28 % to 46 %. Through in-situ calcination, the framework-associated Al formation was inhibited.

## 2. Experimental Section

### 2.1 Catalyst Preparation

HMOR was prepared from commercial Na-form MOR (Yangzhou Zhonghe Petrochemical Institute Co., Ltd.). Typically, the commercial zeolite was stirred in 0.5 mol/L $NH_4NO_3$ solution (Damao Chemical Reagent) at 353 K for 6 h. The suspension was then filtered and washed with deionized water and dried overnight at 383 K, the process is repeated twice to obtain $NH_4$-form MOR. Finally, the sample was calcined at 773 K (2 K/min) for 4 h to obtain H-MOR. Further chemical treatment with ethylenediaminetetraacetic acid disodium salt (EDTA-2Na) was performed on H-MOR.

In a typical run, 5 g of HMOR was suspended in 100 mL EDTA-2Na salt solution (0.05 mol/L) at 358 K and well-mixed for 6, 12, 18, 24 and 36 hours respectively followed by filtration and washing with deionized water. Then ion exchange was performed using $NH_4NO_3$ solution (0.5 M) at 353 K for 6 h, followed by filtration, washing, and drying overnight at 383 K to obtain $NH_4$-MOR-EDTAx (x=6, 12, 18, 24, 36). Finally, H-form MOR was obtained by calcination at 773 K for 4 h, marked as HMOR-EDTAx (x=6, 12, 18, 24, 36).

To test the effect of framework-associated Al on the DME carbonylation reaction, the in-situ calcination method was employed. HMOR-in situ and HMOR-EDTA24-in situ was obtained by calcining $NH_4$-form sample with 10 % $O_2/N_2$ in reactor at 773 K for 4 h. After calcination, the catalyst was evaluated in the reactor.

To further confirm the Al species information of HMOR and HMOR-EDTA24, two additional ammonium ion-exchange were performed on both samples with the same procedure as before. The samples after ammonia ion-exchange were named HMOR-$NH_4$ and HMOR-EDTA24-$NH_4$.

## 2.2. Catalysts Characterization

$^{27}$Al magic angle spinning nuclear magnetic resonance ($^{27}$Al MAS NMR) was performed on a Varian Infinityplus-300 spectrometer operating at a magnetic field of 7.0 T magnet. The resonance frequency during the test was 104.2 MHz, the rotation speed is 8 kHz, and the chemical shift is calibrated with aluminum nitrate standard solution.

X-ray diffraction (XRD) measurement was carried out using a Rigaku D/MAX-

2500, using Cu Kα characteristic diffraction radiation (λ = 0.154 nm, 40 kV, 200 mA), the scanning range was 5~50 °, and the scanning speed was 8 °/min.

Using inductively coupled plasma optical emission spectrometry (ICP-OES) (VISTA-MPX, Varian) to acquire the total content of Si and Al. Before the test, all samples were dissolved in HF solution and then complexed with an excess of $H_3BO_3$.

Nitrogen adsorption measurements were performed at 77 K on a Micromeritics ASAP-2460 analyzer. Before the test, samples (100 mg) were degassed under high vacuum condition at 573 K for 24 h to remove the adsorbed water and other impurities from the sample. The total pore volume and median pore width were determined by the Horvath-Kawazoe (H-K) equation. The total specific surface area of the sample was calculated by the Brunauer-Emmett-Teller (BET) equation, and the micropore surface area and micropore volume were calculated using the t-plot method.

The images of the different samples are acquired by a scanning electron microscopy instrument. (SEM, Apreo S LoVac, FEI, Czech)

Temperature-programmed desorption of ammonia ($NH_3$-TPD) was carried out on a Micromeritics Autochem II 2920 instrument equipped with a thermal conductivity detector (TCD). The sample was pretreated at 473 K for 1 h under an Ar atmosphere to remove impurities. The temperature was then lowered to 423 K and the 10 % $NH_3$/He mixture was introduced to ensure saturation of adsorption. Then samples were purged with He for 1 h to completely remove the physically adsorbed $NH_3$, and then cool down to 373 K. After the baseline was stable, the temperature was then increased from 373 K to 1173 K at 10 K/min. The signal of $NH_3$ was recorded by TCD during the desorption

process.

To selectively determine BAS in 12-MR, Fourier Transform infrared spectroscopy of pyridine adsorption (Py-IR) was also performed on Thermo Scientific Nicolet 6700. Prior to the measurements, samples were pretreated in in-situ cell at 673 K in vacuum for 1 hour. After the pretreatment, the temperature was cooled down to 423 K under vacuum to obtain the background spectrum. Then, the excess pyridine saturated vapor was brought into the in-situ cell by Helium, and the static adsorption was carried out for 30 min. After vacuuming for 30 min to remove the gaseous and weakly adsorbed pyridine molecule, the spectrum was collected with a resolution of 4 $cm^{-1}$ and 32 scans.

## 2.2. Catalytic Performance Evaluation

The reaction for DME carbonylation was carried out in a stainless steel fixed-bed reactor whose inner diameter was 8 mm. The pressure in the reactor was maintained by a back-pressure regulator. Typically, 500 mg catalyst (40-60 mesh) was loaded on the middle of the stainless reactor. The catalyst was pretreated with $N_2$ at 473 K for 9 h. After the pretreatment, the reactant mixture (DME/CO = 1: 49, vol: vol) was introduced into the reactor with a flow rate of 50 mL/min and the reaction pressure was 1.5 MPa. The product was analyzed by an online gas chromatograph (Agilent 7890B), which was equipped with a thermal conductivity detector (TCD) and a flame ionization detector (FID). The conversion of DME ($X_{DME}$) and selectivity to MA ($S_{MA}$) were calculated using equations employed in previous study [21].

## 3. Result and discussion

### 3.1. Physicochemical Characterization

Figure 1 shows the XRD patterns of different samples, all samples had sharp and symmetrical MOR characteristic diffraction peaks, indicating a high crystallinity of all the samples. The relative crystallinity of all samples is listed in Table 1, the crystallinity of HMOR was assumed to be 100 % and the relative crystallinity of EDTA-2Na treated catalyst was calculated based on five most intense peak (2θ=9.8°, 19.6, 22.3°, 25.7°, and 26.3°) [22]. This result suggested that treatment with EDTA-2Na on HMOR did not destroy the zeolite framework, and led to a slight increment in relative crystallinity [23].

The $N_2$ adsorption-desorption isotherms (Figure S1) of the samples were employed to characterize the porous structure for all the samples. Table 1 summarizes the structural parameters of synthesized MOR with different EDTA-2Na treatment time. A series of MOR with different EDTA-2Na treatment time had similar specific surface area, and the micropore and mesopore volume remain constant throughout all the samples. Figure S2 shows the SEM images of all samples. The results showed that all catalysts are constructed by rod stacks, illustrating that the EDTA-2Na treatment did not change the morphology of the catalysts.

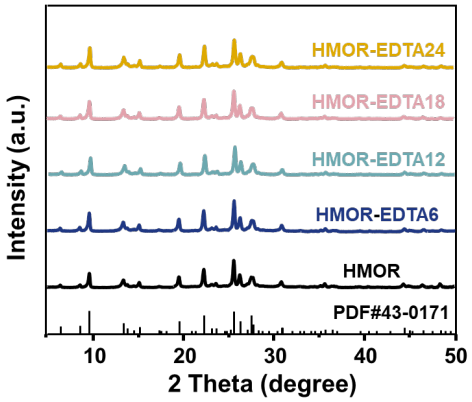


Figure 1. XRD patterns of different samples

Table 1. The textural properties of samples

| Sample | BET Surface Area ($m^2/g$) | Micropore Surface Area ($m^2/g$) | External Surface Area ($m^2/g$) | Micropore Volume ($cm^3/g$) | Mesoporous Volume ($cm^3/g$) | Relative Crystallinity (%) |
|---|---|---|---|---|---|---|
| HMOR | 538 | 527 | 11 | 0.20 | 0.02 | 100 |
| HMOR-EDTA6 | 545 | 525 | 20 | 0.20 | 0.01 | 101 |
| HMOR-EDTA12 | 548 | 528 | 20 | 0.20 | 0.03 | 102 |
| HMOR-EDTA18 | 546 | 527 | 19 | 0.20 | 0.03 | 102 |
| HMOR-EDTA24 | 542 | 526 | 16 | 0.20 | 0.03 | 103 |

As shown in Figure 2, $^{27}Al$ MAS NMR was utilized to identify the aluminum coordination within the parent catalyst and EDTA-2Na-treated sample with the highest DME conversion (HMOR and HMOR-EDTA24). Both the two samples presented two characteristic peaks located at 56 ppm and 0 ppm which are corresponding to tetrahedrally coordinated aluminum (Al(IV)) and hexacoordinated aluminum (Al(VI)) respectively [10, 24]. Though most literature attributes the peak at 0 ppm to EFAl, the framework-associated Al was also reported to contribute to the peak at the same chemical shift [25, 26]. In order to distinguish these two types of Al species, HMOR and HMOR-EDTA24 were treated by ammonia ion-exchange, which are capable of

converting hexacoordinated framework-associated aluminum into tetrahedrally coordinated framework aluminum (Scheme 1). This phenomenon was found in other zeolites as well [20, 27-30]. Figure 2 shows that the resonance peak at 0 ppm of HMOR-$NH_4$ is almost diminished compared to that of HMOR. The relative ratio between Al(IV) and Al(VI) species was calculated by integrating the peak area of NMR results where the HMOR sample showed 21.7 % of Al(VI), whereas the percentage of Al(VI) of HMOR-$NH_4$ decreased to 5.9 % which believed to be EFAl (Table 2). This indicates that the parent HMOR contains a certain amount of EFAl. Similar analysis was applied to EDTA-2Na treated HMOR, the NMR result shows that Al(VI) in HMOR-EDTA24 was 17.7 %, which was smaller than that in the parent HMOR. After being subjected to an additional ammonia ion-exchange process, the HMOR-EDTA24-$NH_4$ shows no peak at 0 ppm (Figure 2), demonstrating that this sample presents neither EFAl nor framework-associated Al. Furthermore, the NMR results clearly illustrate that EDTA-2Na treatment is an efficient way to remove EFAl species. The successful removal of EFAl can be supported by the increase of Si/Al ratio after EDTA-2Na treatment (Table S1). Therefore, $^{27}$Al MAS NMR indicates that HMOR originally had framework-associated Al and EFAl, whereas HMOR-EDTA24 contained only framework-associated Al. As the framework-associated Al is usually produced by the reaction of framework Al with water even at room temperature, we calcinated the $NH_4$-form samples in-situ right before DME carbonylation reactivity evaluation. The samples were noted as HMOR-in situ and HMOR-EDTA24-in situ. In-situ calcination prevents the framework Al from being exposed to air in contact with water to generate

framework-associated Al. XRD, $N_2$ adsorption, and SEM results evidenced that HMOR-EDTA24-in situ also had well-defined crystal phase, pore structure and similar morphology as HMOR-in situ. (Figure S1-3, Table S2)

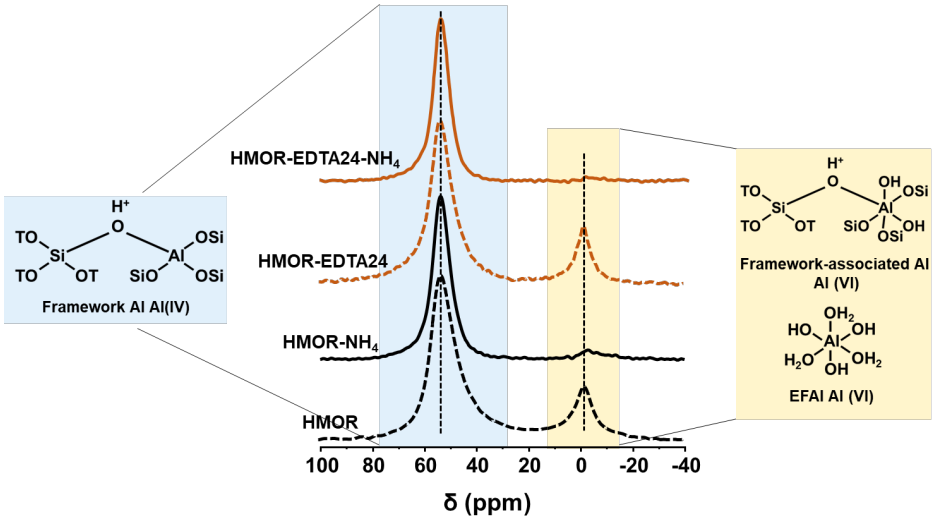


Figure 2. $^{27}$Al MAS NMR spectra of different MOR zeolites.

Table 2. The proportion of Al(IV) and Al(VI) in different samples

| Sample | Al(IV)/ % | Al(VI)/ % |
|---|---|---|
| HMOR | 78.3 | 21.7 |
| HMOR-$NH_4$ | 94.1 | 5.9 |
| HMOR-EDTA24 | 82.3 | 17.7 |
| HMOR-EDTA24-$NH_4$ | 100 | n.d. |

## 3.2. Acid Site Characterization.

It is reported that the conversion of DME is linearly correlated with the number of BASs in 8-MR [7]. In order to study the effect of changes in Al species on the amount of BASs, we used pyridine and ammonia to detect and quantify the number of BASs within different MOR channels. Pyridine with kinetic molecular size of 5.8 Å is unable to access the smaller 8-MR side pocket, while $NH_3$ with a smaller kinetic diameter (2.6

Å) can detect the acid sites within both 8-MR and 12-MR [7, 31, 32].

The peaks at 1540 and 1450 $cm^{-1}$ in IR related to pyridine adsorption at the Brønsted and Lewis acid sites (LASs) [33, 34]. As shown in Table 3, the number of BAS ($BAS_{12\text{-}MR}$) and LAS ($LAS_{12\text{-}MR}$) for 12-MR were calculated using the extinction coefficients from previous study [35]. The profiles of $NH_3$-TPD had three predominate $NH_3$ desorption peaks around 493 K, 570 K, and 753 K corresponding to $NH_3$ desorption from weak, moderate and strong acid sites, respectively. And according to previous studies, the third desorption peak around 753 K is associated with $NH_3$ desorption from Brønsted acid sites [21, 36]. Therefore, the total amount of BAS ($BAS_{total}$) was calculated from the peak area at 753 K (Table 3). The number of Brønsted acid sites in 8-MR ($BAS_{8\text{-}MR}$) is obtained by subtracting $BAS_{12\text{-}MR}$ from $BAS_{total}$. The number of BASs in 12-MR and 8-MR increased and the number of LASs in 12-MR decreased with prolonged EDTA-2Na treatment. As demonstrated above, EDTA-2Na treatment successfully eliminated EFAl. This result indicates that EFAl originally covered the BASs of samples and more BASs were exposed as the removal of EFAl. The slight increase in the number of LASs in 12-MR may be caused by the exposure of the originally covered framework-associated Al after the removal of EFAl by the treatment of EDTA-2Na. In addition, after in-situ calcination, the number of BASs in 12-MR and 8-MR increased and the number of LASs in 12-MR decreased for both HMOR-in situ and HMOR-EDTA24-in situ. Moreover, in-situ calcination improved the BASs within 8-MR more significant than that within 12-MR. This selective promotion of BASs in different channel may be due to the original framework-associated Al

located in 8-MR [25]. Previous work has shown that framework-associated Al is converted to Lewis acid sites at evaluation temperature [10], the results demonstrated that the in-situ calcination could lower the Lewis acidity of samples. Therefore, formation of framework-associated Al can be inhibited by in-situ calcination. Under a similar Si/Al, the inhibition of framework-associated Al formation retains more framework Al, exhibiting considerable Brønsted acidity.

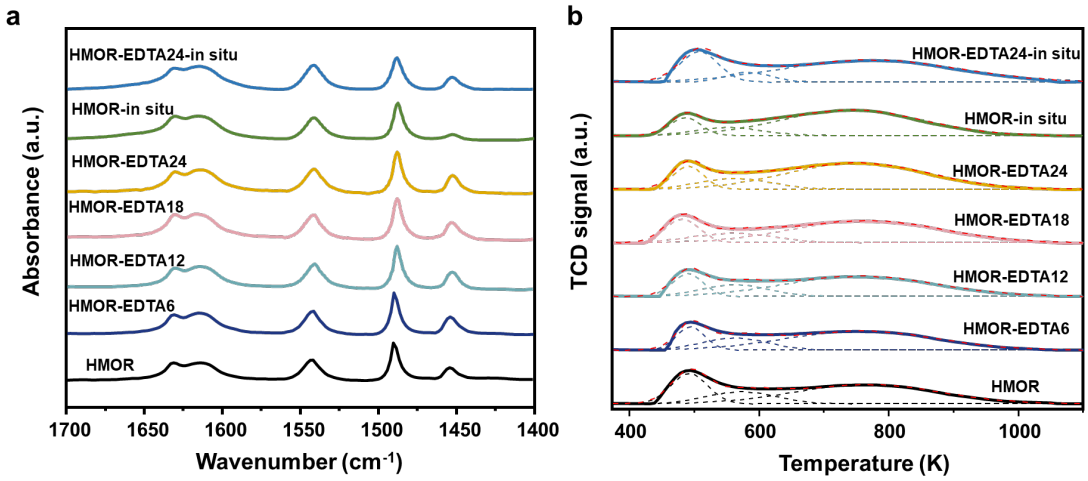


Figure 3. (a) Pyridine-IR spectra profiles, (b) $NH_3$-TPD of samples

Table 3. The number of acid sites in samples

| Sample | $BAS_{total}$[a] (μmol·g$^{-1}$) | $BAS_{12\text{-}MR}$[b] (μmol·g$^{-1}$) | $LAS_{12\text{-}MR}$[b] (μmol·g$^{-1}$) | $BAS_{8\text{-}MR}$[c] (μmol·g$^{-1}$) |
|---|---|---|---|---|
| HMOR | 1071 | 348 | 88 | 723 |
| HMOR-EDTA6 | 1126 | 382 | 137 | 744 |
| HMOR-EDTA12 | 1191 | 394 | 131 | 797 |
| HMOR-EDTA18 | 1302 | 400 | 134 | 902 |
| HMOR-EDTA24 | 1336 | 405 | 128 | 931 |
| HMOR-in situ | 1306 | 378 | 46 | 928 |
| HMOR-EDTA24-in situ | 1472 | 436 | 104 | 1036 |

a: calculated based on $NH_3$-TPD; b: calculated based on Py-IR; c: $BAS_{8\text{-}MR}=BAS_{Total}$ - $BAS_{12\text{-}MR}$

### 3.3. Catalytic Performance for DME Carbonylation

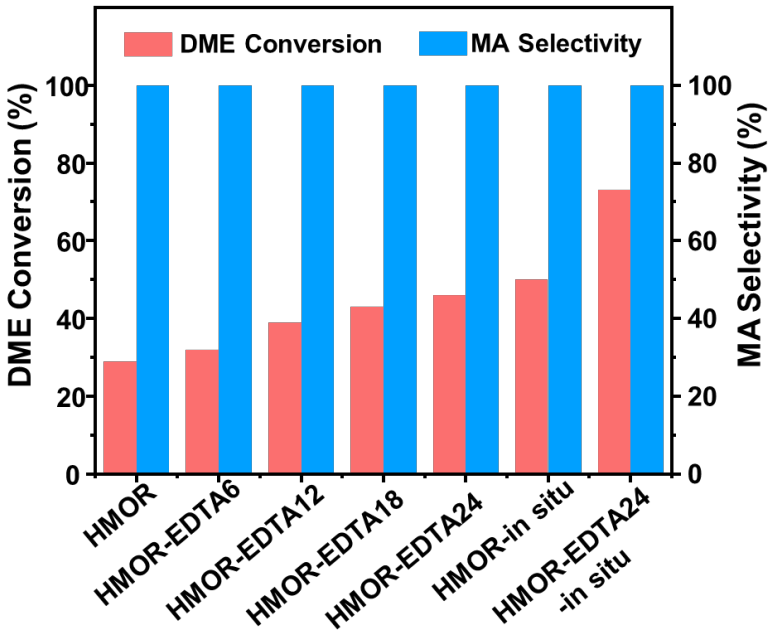


Figure 4. Catalytic performance of different MOR samples (TOS=2.5 h).

Reaction conditions: T=200 °C, P=1.5 MPa, DME/CO=1/49, GHSV= 3000 $h^{-1}$

On the basis of Al coordination and acidity analysis, the influence of EDTA-2Na treatment and in-situ calcination on DME carbonylation reactivity was evaluated. The DME conversion versus time on stream are shown in Figure S4. As reaction time prolonged, the DME conversion increased first and reached the highest value at 2.5 h, then gradually decreased due to the coke formation on BASs in 12-MR. We present the DME conversion and MA selectivity on different MOR catalysts (time on stream=2.5 h) in Figure 4, the MA selectivity higher than 99 % was observed with all the samples, due to the excellent confinement effect of 8-MR in MOR. The HMOR without any pretreatments presented about 28 % DME conversion. And DME conversion kept being promoted with longer EDTA-2Na treatment time, reaching a maximum conversion of

46 % at 24 h of treatment time. There was no increment in the DME conversion when the treatment time was extended to 36 h (Figure S5). The above acidity analysis had proved that the EDTA-2Na treatment could successfully remove EFAl leading to more BASs exposed. Thus, the activity results illustrated that EDTA-2Na treatment was an efficient method to promote carbonylation reactivity through altering the number of exposed active sites.

Compared to the parent catalyst, the in-situ calcination treated MOR sample presented a promotion of DME conversion from 28 % to 50 %. The sample treated with EDTA-2Na and calcined in-situ (HMOR-EDTA24-in situ) showed the highest DME conversion of 73 %, which was about 2.5 times higher in MA formation rate compared to the parent HMOR. The Al coordination and acidity property have substantiated that the in-situ calcination could inhibit framework-associated Al formation and gave rise to the number of BASs in 8-MR. So this promotion of DME conversion demonstrated that the in-situ calcination could be utilized to control the Al species and further highly influence on the reactivity of targeted reactions.

We used two convenient methods to regulate Al species in the catalyst, catalysts were treated with EDTA-2Na to remove EFAl and in-situ calcination was used to inhibit the formation of framework-associated Al. Using both methods to improve DME carbonylation performance, the combination of EDTA-2Na treatment for 24 hours and in-situ calcination resulted in the highest catalytic performance.

## 4. Conclusion

In this work, we elucidated the role of different Al species on the DME

carbonylation reactivity. Through EDTA-2Na post-treatment and adjustment of calcination condition, the removal of EFAl and the inhibition of framework-associated Al formation was achieved. Combined with $^{27}$Al MAS NMR, Py-IR, and $NH_3$-TPD, the results showed an increase in the amount of framework Al and a significant increase in the amount of BASs in 8-MR after the removal of EFAl and the inhibition of framework-associated Al. The DME carbonylation reactivity results illustrate that by EDTA-2Na and in-situ calcination treatment, the DME conversion could be promoted from 28 % to 73 % with MA selectivity of higher than 99 %. This work showed the role of various Al species play in influencing carbonylation reaction through controlling the amount of Brønsted acid sites. This study provides a strategy to modify the Brønsted acidity of zeolite by modulating the Al species and inspires the rational design and improvement of zeolite catalysts in the industrialized catalyzed process.

## Acknowledgement

This work was supported by the National Key Research and Development Program of China (2023YFB4103600) and the National Natural Science Foundation of China (21978209, 22008177).

## References


[1] X. Li, X. San, Y. Zhang, T. Ichii, M. Meng, Y. Tan, N. Tsubaki, ChemSusChem 10 (2010) 1192-1199.

[2] X. San, Y. Zhang, W. Shen, N. Tsubaki, Energy Fuel 5 (2009) 2843-2844.

[3] G. Yang, X. San, N. Jiang, Y. Tanaka, X. Li, Q. Jin, K. Tao, F. Meng, N. Tsubaki, Catal. Today 1 (2011) 425-428.

[4] D. Wang, G. Yang, Q. Ma, Y. Yoneyama, Y. Tan, Y. Han, N. Tsubaki, Fuel 109 (2013) 54-60.

[5] K. Cai, Y. Li, H. Shen, Z. Cheng, S. Huang, Y. Wang, X. Ma, Front. Chem. Sci. Eng. 2 (2021) 319-329.

[6] P. Cheung, A. Bhan, G.J. Sunley, E. Iglesia, Angew. Chem., Int. Ed. 10 (2006) 1647-1650.

[7] A. Bhan, A.D. Allian, G.J. Sunley, D.J. Law, E. Iglesia, J. Am. Chem. Soc. 16 (2007) 4919-4924.

[8] Z. Yu, A. Zheng, Q. Wang, L. Chen, J. Xu, J.P. Amoureux, F. Deng, Angew. Chem. Int. Ed. 46 (2010) 8839-8843.

[9] R.D. Shannon, K.H. Gardner, R.H. Staley, J. Phys. Chem. 89 (1985) 4778-4788.

[10] M. Ravi, V.L. Sushkevich, J.A. van Bokhoven, Nat. Mater. 10 (2010) 1047-1056.

[11] D.L. Bhering, A. Ramírez-Solís, C.J.A. Mota, J. Phys. Chem. B 18 (2003) 4342-4347.

[12] J.A. van Bokhoven, D.C. Koningsberger, P. Kunkeler, H. van Bekkum, A.P.M. Kentgens, J. Am. Chem. Soc. 51 (2000) 12842-12847.

[13] T.N. Pham, V. Nguyen, B. Wang, J.L. White, S. Crossley, ACS Catal. 12 (2021) 6982-6994.

[14] W. Wang, W. Zhang, Y. Chen, X. Wen, H. Li, D. Yuan, Q. Guo, S. Ren, X. Pang, B. Shen, J. Catal. 362 (2018) 94-105.

[15] R. Gounder, A.J. Jones, R.T. Carr, E. Iglesia, J. Catal. 286 (2012) 214-223.

[16] S. Schallmoser, T. Ikuno, M.F. Wagenhofer, R. Kolvenbach, G.L. Haller, M. Sanchez-Sanchez, J.A. Lercher, J. Catal. 316 (2014) 93-102.

[17] M.M. Pereira, F.M. Santos, A.V. Silva, N. Batalha, F.J.F.S. Henrique, P.M. Esteves, B. Louis, J. Phys. Chem. C 21 (2021) 11636–11647.

[18] I.J. Drake, Y. Zhang, M.K. Gilles, C.N.T. Liu, P. Nachimuthu, R.C.C. Perera, H. Wakita, A.T. Bell, J. Phys. Chem. B 24 (2006) 11665-11676.

[19] L.C. Ménorval, W. Buckermann, F. Figueras, F. Fajula, The Journal of Physical Chemistry 1996 2 (1996) 465-467.

[20] B.H. Wouters, T.H. Chen, P.J. Grobet, J. Am. Chem. Soc. 44 (1998) 11419-11425.

[21] M Wang, S Huang, J Lv, Z Cheng, Y Li, S Wang, X Ma, Chin. J. Catal. 9 (2016) 1530-1537.

[22] K. Cai, S. Huang, Y. L, Z. Cheng, J. Lv, X. M, ACS Sustainable Chem. Eng. 7 (2018) 2027-2034.

[23] J.L. Agudelo, B. Mezari, E.J.M. Hensen, S.A. Giraldo, L.J. Hoyos, Appl. Catal. A Gen. 488 (2014) 219–230.

[24] S.R. Batool, V.L. Sushkevich, J.A. van Bokhoven, J Catal. 408 (2022) 24-35.

[25] M. Ravi, V.L. Sushkevich, J.A. van Bokhoven, Chem. Sci. 12 (2021) 4094-4103.

[26] M. Ravi, V.L. Sushkevich, J.A. van Bokhoven, J. Phys. Chem. C 123 (2019) 15139-15144.

[27] E. Bourgeat-Lami, P. Massiani, F. Di Renzo, P. Espiau, F. Fajula, T. Des Courières, Appl. Catal. 1 (1991) 139-152.

[28] B. Gil, S. I. Zones, S. Hwang, M. Bejblová, J. Čejka, J. Phys. Chem. C 8 (2008) 2997–3007.

[29] G.L. Woolery, G.H. Kuehl, H.C. Timken, A.W. Chester, J.C. Vartuli, Zeolites 4 (1997) 288-296.
[30] J.A. van Bokhoven, A.M.J. Eerden, D.C. Koningsberger, J. Am. Chem. Soc. 24 (2003), 7435-7442.
[31] S. Bordiga, C. Lamberti, F. Bonino, A. Travert, F. Thibault-Starzyk, Chem. Soc. Rev. 20 (2015) 7262-7341.
[32] X. Liu, Y. Pan, P. Zhang, Y. Wang, G. Xu, Z. Su, X. Zhu, F. Yang, Front. Chem. Sci. Eng. 16 (2022) 384-396.
[33] Y. Li, Q. Sun, S. Huang, Z. Cheng, K. Cai, J. Lv, X .Ma, Catal. Today 311 (2018) 81-88.
[34] Y. Li, Z. Li, S. Huang, K. Cai, Z. Qu, J. Zhang, Y.Wang, X. Ma, ACS Appl. Mater. Interfaces 27 (2019) 24000-24005.
[35] C.A. Emeis, J. Catal. 2 (1993) 347-354.
[36] Y. Liu, N. Zhao, H. Xian, Q. Cheng, Y. Tan, N. Tsubaki, ACS Appl. Mater. Interfaces 16 (2015) 8398-8403.